Physics Basis of ITER-FEAT

M. Shimada 1), D. J. Campbell 2), M. Wakatani 3), H. Ninomiya 4), N. Ivanov 5),
V. Mukhovatov 1) and the ITER Joint Central Team and Home Teams

1) ITER Joint Central Team, Naka Joint Work Site, Naka-machi, Ibaraki-ken, Japan
2) EFDA Close Support Unit, Garching, Germany
3) Kyoto University, Kyoto, Japan
4) Japan Atomic Energy Research Institute, Naka-machi, Ibaraki-ken, Japan
5) Kurchatov Institute, Moscow, Russian Federation

e-mail contact of main author: shimadm@itergps.naka.jaeri.go.jp

Abstract. This paper reviews Physics R&D results obtained since the publication of the ITER Physics Basis document. The heating power required for the LH transition has been re-assessed, including recent results from C-Mod and JT-60U and it has been found that the predicted power is a factor of two lower than the previous projection. For predicting ITER-FEAT performance, a conservative scaling IPB98(y,2) has been adopted for the energy confinement, producing confinement times ~ 20 % lower than those derived from the IPB98(y,1) law. While energy confinement degradation at high density remains a serious issue, recent experiments suggest that good confinement is achievable in ITER at $n/n_G \sim 0.85$ with high triangularity. The estimated runaway electron energy has been reduced to ~ 20 MJ, since recent experiments show that runaway electrons disappear for $q_{95} \leq 2$.

1. Introduction

The performance projections for ITER have been made according to the methodologies described in the ITER Physics Basis document (IPB) [1], some of which have been updated according to the recent Physics R&D. This paper reviews Physics R&D results obtained since the publication of the IPB.

2. H-mode scalings

The recommended form for the H-mode power threshold scaling [2] is,

$$P_{\mathrm{LH}} = 2.84 M^{-1} B_{\mathrm{T}}^{0.82} \bar{n}_{\mathrm{e}}^{0.58} R^{1.00} a^{0.81} \qquad \text{(rms err. 0.268)} \qquad (1)$$

in (MW, AMU, T, 10^{20}m^{-3}, m), with M the effective isotopic mass of the plasma fuel. This scaling expression is based on the latest version of the threshold database (DB3) including results from recent dedicated H-mode threshold experiments in Alcator C-Mod and in JT-60U [2], the latter using the new 'W' shaped divertor. For ITER-like devices, this scaling yields an H-mode power threshold prediction which is approximately a factor of 2 lower than that predicted by an earlier version IPB98(5).

Thermal energy confinement in the ELMy H mode is described by the IPB98(y,2) scaling,

$$\tau_{E,th}^{IPB98(y,2)} = 0.0562 I_p^{0.93} B_T^{0.15} P^{-0.69} n_e^{0.41} M^{0.19} R^{1.97} \varepsilon^{0.58} \kappa_a^{0.78} \qquad \text{(rms err. 0.145)} \qquad (2)$$

where the units are (s, MA, T, MW, 10^{19}m^{-3}, AMU, m) and κ_a is the plasma elongation defined as $\kappa_a = S_o/\pi a^2$ with S_o being the plasma cross-sectional area. A comparison of the H-mode thermal energy confinement times ($\tau_{E,th}$) with the scaling (2) for a subset of ELMy data in the ITER H-mode database is shown in Fig. 1. Also shown is the IPB98(y,2) scaling prediction for $\tau_{E,th}$ in a nominal ITER-FEAT Q = 10 discharge. In the IPB report [1], five empirical log-linear (power law) scaling expressions for $\tau_{E,th}$ are presented. IPB98(y,2) has been selected as a conservative option.

The maximum density at which high confinement can be sustained is a critical issue. Although it has traditionally been difficult to maintain H-mode confinement at densities close to the Greenwald value, experiments at higher triangularity in JET [3] have obtained H-mode quality confinement at 80% of the Greenwald density. In addition, experiments with inside pellet launch in ASDEX Upgrade [4] and recent experiments in DIII-D with pumping at both the inboard and outboard divertor strike points [5] have sustained H-mode level confinement at densities beyond the Greenwald value.

Figure 2 plots experimental $\tau_{E,th}$ normalised by (y,2) scaling ($H_{y,2}$) vs. electron density normalised by Greenwald density, showing many points $H_{y,2} \sim 1$ around $n/n_G \sim 0.85$. In addition, deterioration of confinement would be avoided in ITER at a lower density operation, typically $n/n_G = 0.7$. The operation space for low density Q = 10 operation would be expanded with ion heating by ICRF and/or low edge density with pellet injection [6].

High-Field-Side pellet injection exhibits penetration superior to Low-Field-Side injection. Grad-B drifts and subsequent ExB drift are proposed as a potential mechanism [7,8], but a model including ablation and penetration has yet to be developed.

3. ITB and Steady state

Non-inductive steady-state operation requires challenging values of $H_{y,2} \sim 1.5$ and $\beta_N \sim 3.0$-3.5 as well as high bootstrap (BS) current fraction. It is considered that weakly reversed shear (RS) or optimised shear operation with internal transport barrier (ITB) may offer scenarios satisfying these requirements.

Different power thresholds for ITB formation have been obtained experimentally. JET experiments show the importance of target q_o and increase in threshold power with toroidal field. JT-60U experiments with strong RS show a weak dependence on toroidal field and density and the ITB threshold power approximately the same as the H-mode threshold power.

Significant progress in increasing the duration of the high performance phase of discharges with ITBs has been achieved recently in JT-60U, JET, DIII-D and TORE Supra. A weak RS mode with ITB and ELMy H-mode edge has been sustained in JT-60U for 2.6 s with $\beta_N \cong 2.5$, $H_{89P} \cong 2.5$, $H_{y,2} = 1.7$, $q_{95} \sim 4.1$ and non-inductively driven current fraction of 70-80% (ratio of BS current fraction to NB driven current fraction $f_{BS}/f_{NB} \approx 2/1$)[9]. A 2 s discharge phase with strong RS and BS current fraction of 70% (total non-inductively driven fraction ≅ 90%) at $\beta_N \cong 1.9$-2.1 and $H_{89P} \cong 2.8$-3.4 has been obtained. Also, a fully non-inductive RS discharge with ITB has been sustained for 5 s in JT-60U with a LHCD fraction of 77% and BS current fraction of 23% although at relatively low $\beta_N \cong 1$. The product $\beta_N H_{89P}$ has been maintained up to 7.3 for several confinement times in JET using an argon impurity-seeded edge, although impurity accumulation within the ITB has been observed possibly due to a peaked plasma density profile [10]. The high performance phase of the ELMy H-mode with $\beta_N \cong 3.5$ ($\cong 4\ l_i$), $H_{89P} \cong 2.6$ and BS current fraction of 50% was sustained for 2 s ($\sim 16\tau_E$) in DIII-D [11]**.** The product $\beta_N H_{89P} = 7.2$ was sustained at $q_{95} = 4.5$ for 40 confinement times and 2.5 resistive time scales for internal current redistribution in ASDEX Upgrade [12].

Although significant progress has been achieved in obtaining and sustaining ITBs in current experiments, projections of such regimes to reactor conditions can not be done reliably yet. The role of the external toroidal momentum input, density profile and T_i/T_e in ITB formation remains unclear. Although ion thermal transport can be reduced to the neoclassical level

within ITBs, the electron transport in some cases remains anomalous. All high performance discharges with ITBs obtained so far have relatively low plasma densities, $n_e \leq 0.65\ n_G$ while $n_e \sim n_G$ will be required in a reactor. Successful steady-state operation with enhanced core confinement and high BS fraction demands developing the control tools for current profile control, ELM control, neoclassical tearing modes (NTM) and resistive wall modes (RWM) control and plasma pressure profile control. Theories are emerging for ITB formation; suppression of ITG and ETG turbulence in negative magnetic shear, and suppression of turbulence by zonal flow. The Weiland-Nordman transport model is shown to be applicable to ASDEX Upgrade plasmas with combined NB and ECR heating when $T_e \geq T_i$ [13].

Reasonable current drive (CD) efficiencies are obtained for on-axis and near off-axis CD for NB, IC and EC. Recently, JT-60U achieved 1.55 x 10^{19} A/W/m^2 for N-NBI at 366 keV at central electron temperature of 12.7 keV [14]. Transport calculation of ITER indicates the need of far off-axis CD in the case of a flat density profile. This scenario would be feasible only with LHCD, because CD efficiency is low in other CD methods. A sufficient density gradient far off-axis would eliminate the need of far off-axis CD [15].

For the long pulses (> 1000 s) in ITER, problems may arise with the measurement of plasma shape and position by magnetics particularly due to a small emf which tests have shown may be induced by radiation. In addition, a reliable method needs to be developed for q profile measurement [16,17].

4. Pedestal and ELM

Cross-machine comparison suggests that the pedestal width is proportional to ion poloidal Larmor radius, but the proportionality coefficients are different from one machine to another. A new model for the H-mode pedestal (edge) width is proposed based on turbulence suppression by the combined effects of the magnetic and $\boldsymbol{E} \times \boldsymbol{B}$ shear [18]. Its comparison against C-Mod and JET data is encouraging, albeit the model uses magnetic shear which is not measured in experiments and the density profile data is not available in C-Mod. The shrinking of pedestal layer at high density and consequent reduction of core temperature may offer a possible explanation for the deterioration of confinement.

The present ELM scaling predicts that the divertor heat load associated with type I ELMs might be unacceptably high. However, this database was taken from discharges with low Greenwald numbers (~ 0.4). ELMs with reduced amplitudes were observed in DIII-D in a high density regime (pedestal density/$n_G \sim 0.9$) [19]. In this density range, they observed $H_{89P} \sim 1.5$, associated with peaked density profile.

Establishment of an operational scenario with high density, good confinement and tolerable ELMs is an important issue. For high q ($q_{95} \geq 4$) operation, such as non-inductive and hybrid operation, more benign type-II ELMs or an EDA(Enhanced D_α mode) is expected [20]. For inductive operation in ITER, two approaches are possible [6] for reduction of the ELM heat load; (1) Many experiments show that the density is limited at the edge, suggesting that a peaked density profile allows the volume-averaged density to exceed the Greenwald density. Peaked density profiles with HFS pellet injection would enable Q = 10 at lower current (e.g. ≤ 11 MA) satisfying $q_{95} \geq 4$, the condition for type-II ELMs or the EDA. Confinement improvement with pellet injection and ion heating by ICRF would facilitate the achievement of Q = 10. (2) Low fusion power is expected to reduce the ELM heat load. Ion heating by ICRF enables operation at a low fusion power of ~ 200 MW at Q = 10.

5. Divertor

The divertor model validation against experiments has also made progress [21]. Excellent agreement was obtained between the measured and calculated radiation profiles.
A large amount of carbon deposit was observed in the inner divertor in JET and many other tokamaks. Development of erosion/redeposition models and validation with experiments is an important issue, because this problem is related with tritium retention.

6. Ripple reduction

In JFT-2M, ferritic inserts (FI) reduced the toroidal field ripple from 2.2 % to 0.5 %, reducing the ripple-trapped losses significantly [22]. The FI gives no adverse effect on plasma production and control. A Monte-Carlo calculation has been made on ripple particle loss. Without correction of the TF ripple, α particle loss in ITER is small in the inductive mode, but is rather high (2.5% of α heating power or 230 kW/m^2 of the peak heat load at the first wall) in RS mode with $q_{min} = 2$. FI in the vacuum vessel reduces the ripple particle loss sufficiently (0.04% of α heating power and 5 kW/m^2 of the peak heat load at the first wall).

7. Disruptions and beta limits

Disruption remains a critical issue for ITER design, but this area has witnessed a lot of progress recently; schemes either to avoid disruption or mitigate its consequences have been developed and tested. A neural network is powerful for predicting disruption [23], killer pellets can reduce the force and heat loads, and production of runaways is prevented by magnetic fluctuations. Runaway electrons are eliminated completely by wall contact at safety factors q_{eff} of the disrupting core plasma below 2.5 ($q_{95} \leq 2$) [24]. Numerical simulations of ITER suggest that the runaway electron energy probably cannot exceed 20 MJ for a plasma edge density above 2×10^{19} m^{-3} if runaway electrons are lost at $q_{95} \leq 2$.

Remarkable progress was also made in stabilising NTM and RWM. No phased ECCD in the O-points of the NTM islands is needed, but dc CD is sufficient. In ASDEX-Upgrade, a complete stabilisation of (3/2) neoclassical tearing modes with dc ECRH current drive and heating could be achieved [25]. However, there remains uncertainty in predicting the onset beta, determining the influence of shape and the required ECCD power for NTM in ITER. The necessity to stabilise both 3/2 and 2/1 NTMs in ITER cannot be excluded. ITER calculations suggest that the required power for NTM stabilisation can be reduced to 18 MW, if early detection at ~ 1/3 of the saturated island width is possible [26].

Non-inductive operation requires challenging values of $H_{y,2}$ (~ 1.5) and β_N (3.0-3.5). For such an operation, RWM may limit the achievable beta. A complete suppression of RWM and the performance above the no-wall kink limit are yet to be demonstrated. In ITER, the error-field correction coils can be used for feedback stabilisation.

8. Conclusions

Extensive Physics R&D and design efforts have demonstrated that the major issues associated with Q = 10 inductive operation can be resolved. For advanced mode of operations, more efforts are needed in the areas including confinement improvement, current and pressure profile control, resistive wall mode control, tritium inventory control and some diagnostic techniques.

References

[1] ITER PHYSICS BASIS EDITORS, *Nucl. Fusion* **39** (1999) 2137.
[2] SNIPES, J.A., et al., Plasma Phys. Control. Fusion **42** (2000) A299.
[3] SAIBENE, G., et al., Nucl. Fusion **39** (1999) 1133.
[4] LANG, P. T., et al., Phys. Rev. Lett. **79** (1997) 1487.
[5] OSBORNE, T.H., *et al.,* 14th International Conference on Plasma Surface Interactions, May 22-26, 2000, Rosenheim, Germany.
[6] MURAKAMI, Y., et al., this conference.
[7] STRAUSS, H.R., et al., Phys. Plasma **5** (1998) 2676.
[8] PARKS, P.B., et al., Phys. Plasma **7** (2000) 1968.
[9] KAMADA, Y., et al., Plasma Phys. Control. Fusion **42** (2000) A65.
[10] GORMEZANO, C., et al., 27th EPS Conf. on Control. Fusion and Plasma Phys., Budapest, 12-16 June 2000, P1.048.
[11] GREENFIELD, C.M., et al., Phys. Plasmas **7** (2000) 1959.
[12] GRUBER, O., et al., Nucl. Fusion **40** (2000) 1145.
[13] PEREVERZEV, G.V., et al., 27th EPS Conf. on Controlled Fusion and Plasma Phys., Budapest, 12-16 June 2000, P3.046.
[14] OIKAWA, T., et al., this conference.
[15] FUJISAWA, N., et al., this conference.
[16] COSTLEY, A., et al., Rev. Sci. Instrum. **70** (1999) 391.
[17] DONNE, A.J.H., et al., this conference.
[18] SUGIHARA, M., et al., Nucl. Fusion **40** (2000) 1734.
[19] LEONARD, A.W., et al., 14th International Conference on Plasma Surface Interactions, May 22-26, 2000, Rosenheim, Germany.
[20] KAMADA, Y., et al., Plasma Phys. Control. Fusion **42** (2000) A247.
[21] LOARTE, A., et al., J. Nucl. Mat. **166-169** (1999) 1123.
[22] KAWASHIMA, H.K., et al., this conference.
[23] PAUTASSO, G., et al., 14th International Conference on Plasma Surface Interactions, May 22-26, 2000, Rosenheim, Germany.
[24] YOSHINO, R., et al., Nuclear Fusion **39** (1999) 151.
[25] MARASCHEK, M., et al., 27th EPS Conf. on Controlled Fusion and Plasma Phys., Budapest, 12-16 June 2000,OR.008.
[26] PUSTOVITOV, V.D., et al., this conference.

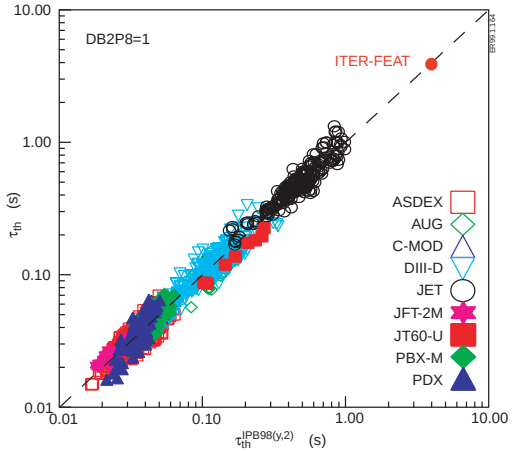

FIG. 1. Comparison of ELMy H-mode $\tau_{E,th}$ with the (y,2) scaling.

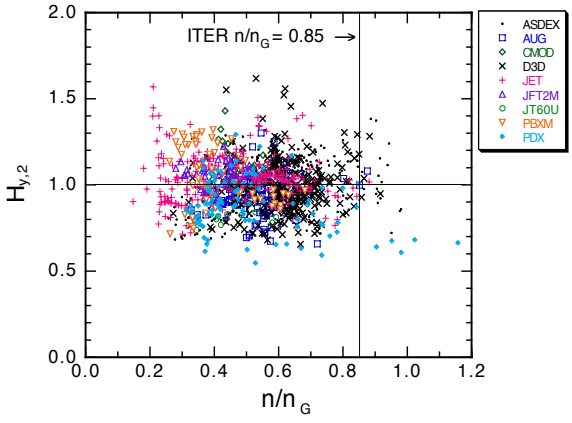

FIG. 2. Experimental $\tau_{E,th}$ normalised by (y,2) scaling vs. normalised density (n/n_G).